

Document downloaded from:

<http://hdl.handle.net/10251/49295>

This paper must be cited as:

Benajes Calvo, JV.; Molina Alcaide, SA.; García Martínez, A.; Monsalve Serrano, J.; Durrett, R. (2014). Conceptual model description of the double injection strategy applied to the gasoline partially premixed compression ignition combustion concept with spark assistance. *Applied Energy*. 129:1-9. doi:10.1016/j.apenergy.2014.04.093.



The final publication is available at

<http://dx.doi.org/10.1016/j.apenergy.2014.04.093>

Copyright Elsevier

20 **ABSTRACT**

21 New combustion concepts applied to Compression Ignition engines are focused on achieve low
22 temperature combustion together with a lean mixture distribution by allowing extra time from the end
23 of injection to the start of combustion. Recently, the use of gasoline in a Compression Ignition engine
24 under PPC conditions has been demonstrated as a suitable technique to achieve this extra mixing time,
25 however the concept has also demonstrated difficulties under low load conditions using gasoline with
26 octane number up to 95. The use of spark assistance with single injection operation has been found to
27 be an appropriate way to improve the combustion control, providing both temporal and spatial control
28 over the combustion process.

29 The current paper details the influence of the double injection strategy on the Spark Assisted Partially
30 Premixed Combustion concept compared with the single injection strategy. For this purpose, a reference
31 combustion cycle for both injection strategies is compared in terms of the main parameters derived
32 from the in-cylinder pressure signal as well as OH* and natural luminosity images acquired from the
33 single-cylinder transparent engine. The cylinder head used along the research has been modified
34 including a spark plug. In addition, a detailed analysis of the air/fuel mixing process has been developed
35 by means of a 1-D in-house spray model.

36 **KEYWORDS**

37 Partially premixed combustion

38 Spark assistance

39 High octane number gasoline

40 Combustion control

41 Double injection

42 Natural luminosity and OH images

43

44 **1. INTRODUCTION**

45 The automotive scientific community and manufacturers are currently focusing part of their efforts on
46 the investigation of new combustion modes [1][2] and on the optimization of the current technology
47 with the aim of reducing fuel consumption and emissions in CI diesel engines [3]. Most of these new
48 combustion concepts are achieved by using different strategies that produce a lean air-fuel mixture
49 together with a low temperature combustion. It contributes to decrease drastically the most relevant CI
50 diesel engine-out emissions, NO_x and soot [4]. In addition, due to the in-cylinder mixture homogeneity,
51 a fast heat release is obtained when the proper in-cylinder conditions are achieved providing high
52 combustion efficiency.

53 These combustion concepts based on fully or partially premixed lean mixtures are commonly known as
54 Homogeneous Charge Compression Ignition (HCCI) [5][6]. Even though they achieve important emission
55 benefits [7], these combustion concepts present some practical issues that must be overcome before
56 they can be implemented in CI diesel engines being confined to low engine speeds and loads [8]. The
57 most relevant limitations of this combustion modes consist of achieving an appropriate combustion
58 phasing, the cycle-by-cycle control of the combustion process, spray impingements and its effects on the
59 emissions [9], the noise and operating range extent. Several techniques such as EGR [10], variable valve
60 timing [11][12], variable compression ratio [13] and intake air temperature variation [14] have been
61 investigated in order to overcome these drawbacks. Due to the high chemical reactivity of the diesel
62 fuel, the mentioned techniques cannot provide precise control over the combustion phasing since they
63 require large time scales to achieve cycle-by-cycle control. Thus, not enough mixing time before the
64 start of combustion is provided.

65 The scientific community is currently trying to overcome these disadvantages by using fuels with
66 different reactivity [15][16][17]. In this sense, Partially Premixed Combustion (PPC) using a low reactivity
67 fuel has been confirmed as promising method to control the heat release rate providing a reduction in

68 NOx and soot emissions as well. The use of a high ON fuel, such as gasoline, in a CI engine under PPC
69 conditions provides more flexibility to reach lean and low combustion temperatures due to the extra
70 mixing time achieved [18] through the fuel properties. However, the concept has demonstrated
71 difficulties at low load conditions using gasoline with octane number greater than 90, concluding that
72 the use of a low reactivity fuel under PPC conditions provide some control on combustion phasing but
73 still do not solve the possibility of cycle-by-cycle control.

74 Recent investigations on gasoline engines (SI) running in homogenous or premixed combustion modes
75 such as CAI (always PFI) [19][20], have shown the potential of using the assistance of a spark plug for
76 achieving cycle-to-cycle control and combustion phasing control. The results suggest that this strategy
77 can provide good combustion phasing while the response time is short enough for cycle-by-cycle
78 application. Nevertheless, further research on spark assistance in new combustion modes is necessary
79 for continuing its development with low reactivity fuels [21][22]. Thus, with the aim of integrating
80 phasing and cycle-to-cycle control by means of a spark plug ignition system in a CI engine working in
81 partially premixed charge, the PPC concept with spark assistance fuelled with gasoline has been studied.
82 This engine architecture has a high compression ratio and it is equipped with a common rail injection
83 system that enables high injection pressures. Thus, the Partially Premixed Combustion concept with
84 Spark Assistance has been evaluated in terms of performance and engine-out emissions using a single
85 injection strategy by studying the effect of injection pressure variations and intake oxygen
86 concentration. Under these conditions, spark assistance has been found to be a suitable technique for
87 improving combustion control, providing both temporal and spatial control over the combustion process
88 [23][24]. In spite of its benefits, some drawbacks related to unappropriated mixture distribution and
89 combustion temperatures are attained. Single injection provides excessive rich zones near to the spark
90 plug and excessive lean regions close to the wall chamber resulting in high emission levels as well as
91 deteriorated fuel energy conversion efficiency. Thus, the main objective of the present work is to

92 analyze the effect of the double injection strategy on the mixture distribution and combustion
93 development under partially premixed compression ignition spark assisted mode. The investigation was
94 performed in an optical engine since it is a suitable tool for performing a basic combustion research
95 combining in-cylinder pressure signal derived parameters and optical combustion images as an
96 experimental sources of information together with a 1-D spray model.

97 The outline of this paper is as follows: in the first section, the experimental facilities and the different
98 setups used to carry out this research are presented. Specifically, this section describes briefly the
99 methodology, experimental facilities and processing tools used from the acquisition of the raw data
100 during the experimental tests to the final results obtained by means of the post-processing tools. In the
101 following section, which is the base of this paper, a summary of the preliminary results and a description
102 of the combustion event comparing the single and double injection strategies are done. Finally, in
103 section 4, the main conclusions of this research are summarized.

104 **2. EXPERIMENTAL FACILITIES AND PROCESSING TOOLS**

105 This section describes the methodology used to acquire the experimental data and provides a
106 description of the experimental facility, the different devices and systems that were specifically adapted
107 for the study of this combustion mode.

108 **2.1 Experimental setup**

109 This section presents the experimental configuration of the test cell and the main subsystems used in
110 this study. As Figure 1 shows, the single cylinder engine is installed in a fully instrumented test cell, with
111 all the auxiliary facilities required for operation and control.

112 The intake air is supplied by a Roots compressor with an upper pressure limit of 3 bar. Then, the air
113 flows through a filter to remove possible impurities. The heat exchanger and the air dryer allow
114 controlling the temperature and humidity of the intake air independently of the ambient conditions. The

115 temperature in the inlet settling chamber is maintained constant by using the heater in the intake line.
116 The oxygen concentration variation is performed using a synthetic EGR system. EGR is substituted by
117 nitrogen gas, which greatly simplifies the system ensuring a controllable gas composition without an
118 excessive time to adjust the facility. Despite the limited practical application, it was decided to use this
119 method to have a better control of the variables, which allows studying the underlying phenomena
120 more carefully. The concept is based on decreasing the O₂ concentration at the inlet manifold by
121 increasing the flow of N₂ and keeping constant the total intake mass flow rate (substitution EGR). For
122 this purpose a PID controller is equipped to operate the N₂ valve governed by the intake O₂ meter. With
123 this system, the in-cylinder thermodynamic conditions can be reproduced systematically. To ensure a
124 homogeneous mixture of N₂ and O₂ and to attenuate pressure pulses in the intake manifold, a settling
125 chamber of 500 liters volume is used in the installation. In the exhaust line, after the exhaust analyzer
126 sample probe, a catalyst is mounted to prevent the accumulation of unburned hydrocarbons in the
127 installation. Due to the low temperatures achieved during the combustion event and therefore in the
128 exhaust line, the catalyst is often operating with low efficiency and a cyclone is needed to remove the
129 rest of the hydrocarbons. In the same way as in the intake line, a settling chamber is mounted in order
130 to attenuate pressure pulses. Finally, an exhaust backpressure valve is equipped to maintain a relative
131 pressure of 0.2 bar to the intake pressure, in order to simulate more realistic conditions.

132 **2.1.1 Engine description and cylinder head adaptation**

133 The engine used in the present study is a 4-valve, 0.545 l displacement single cylinder engine with a
134 modified cylinder head for the study of this combustion mode. The bowl dimensions are 45x18 mm
135 (diameter x depth). Table 1 presents the main characteristics of the engine.

136 In order to characterize the most relevant properties of the gasoline used in this research, various
137 analyses of the fuel properties have been performed following ASTM standards. It is worthy to note that

138 300 ppm of additive (*Havoline Performance Plus*) was added to improve the lubricity of the gasoline up
139 to diesel fuel level, increasing the service life of the high pressure pump and fuel injector. The addition
140 of the additive does not modify neither density nor the viscosity. The results of the gasoline
141 characterization are summarized in Table 2.

142 The fuel injection hardware characteristics are depicted in Table 3. The injection control system allows
143 to modify any parameter of the injection event such as timing, duration and rail pressure.

144 A spark plug is required to implement the partially premixed compression ignition with spark assistance
145 combustion mode. As Figure 2 shows, the cylinder head has been modified by removing an exhaust
146 valve and thus enabling the insertion of the spark plug in the combustion chamber. A standard spark
147 plug (Veru Platinum) with a 1 mm gap is used along with a custom electronic control system. In the
148 standard configuration, the tip protrudes 4.5 mm into the combustion chamber from the cylinder head
149 plane and it is located 17 mm from the cylinder axis. The injector is centered and vertically assembled in
150 the modified cylinder head with a graduated metal circle that can change the relative position between
151 the spark plug and the injector fuel jets by rotating the injector around its vertical axis. This relative
152 position is fixed to make the spray pass between the spark electrodes.

153 In order to increase the reliability of the combustion mode, a Delphi multicharge ignition system has
154 been used. The high amount of energy released by this ignition system allows igniting the mixture even
155 with local equivalence ratio conditions near their flammability limits with high EGR rates. The spark
156 ignition system is operated at a constant nominal primary voltage of 15 V from the battery and primary
157 current of 25 A, providing around 120 mJ for the typical combustion chamber density test conditions,
158 almost double than of a conventional ignition system.

159

160

161

2.1.2 Optical engine configuration

162 The engine is equipped with an elongated piston with a cylindrical bowl, which allows optical access to
163 the combustion chamber through a sapphire window placed in its bottom. Below the piston bowl, an
164 elliptical UV mirror is placed on the cylinder axis. In front of the mirror, a beam splitter (50%-50%) is
165 positioned in order to allow the simultaneous acquisition of the OH radical luminosity and the natural
166 luminosity. For the acquisition of the natural luminosity images, a high speed Phantom V12 CMOS
167 camera equipped with a 100 mm focal length Zeiss lens is utilized with an image resolution of 512 x 512
168 pixels. In order to acquire the OH radical luminosity images a Photron intensified camera equipped with
169 a 100 mm UV lens together with a band pass filter centered at 310 nm is utilized. Figure 3 shows the
170 optical scheme. It is interesting to note that the tests have been performed under skip-fire mode (1
171 cycle fired per 30) in order to avoid excessive thermal stress in the windows and ensure the same in-
172 cylinder initial thermodynamic conditions for the recorded (fired) cycles.

173

2.2 Theoretical tools

174 In order to understand how the results are obtained from the experimental data, a brief description of
175 the principles behind the different tools used for processing and post-processing the results is provided
176 here.

177

2.2.1 Analysis of pressure signal

178 The combustion analysis is performed with an in-house one-zone model named CALMEC, which is fully
179 described in [25]. This combustion diagnosis tool uses the in-cylinder pressure as its main input. The in-
180 cylinder pressure was measured with a Kistler 6067C1 pressure transducer. The pressure traces for 200
181 engine cycles were recorded in order to compensate the cycle-to-cycle variation during engine
182 operation. Then, the first law of thermodynamics is applied between IVC and EVO, considering the

183 combustion chamber as an open system because of blow-by and fuel injection. The ideal gas equation of
184 state is used to calculate the mean gas temperature in the chamber. Along with these two basic
185 equations, several sub-models are used to calculate instantaneous volume and heat transfer [26],
186 among other things. The main result of the model is the Rate of Heat Release (RoHR). Information
187 related to each cycle can be obtained, such as the IMEP and SoC. Start of Combustion (SoC) is defined as
188 the crank angle position in RoHR where the beginning of the slope rise due to combustion is detected.

189 **2.2.2 Analysis of mixing process**

190 A 1-D in-house spray model DICOM is used to estimate equivalence ratio distributions in the fuel jet in
191 order to get better insight into the variations in mixture distribution associated with the variations in the
192 parameters studied in the experimental tests. The start of combustion and the combustion development
193 have an extreme dependency on the local mixture conditions at Start of Spark (SoS) timing. The inputs
194 of the DICOM model are the in-cylinder thermodynamic conditions (pressure, temperature and density),
195 the spray cone angle, the fuel mass flow rate and the spray momentum. The model solves the general
196 conservation equations either in a transient or steady state formulation for axial momentum and fuel
197 mass along the center line. The results can be used to calculate values of spray velocity, species mass
198 fractions and other values of the mixing process [27]. Finally, with some other assumptions described in
199 [28], the model is used to obtain different temporal evolutions such as the spray liquid and vapor
200 penetration, maximum spray velocity, equivalence ratio along the center line of the spray and the fuel
201 mass fraction which has mixed to different equivalences ratios. The fuel mass fraction is the main
202 variable used in this research.

203 **2.2.3 Image processing tool**

204 In order to complement the information about the differences in the combustion development for both
205 injection strategies, time resolved parameters were calculated for every image in each sequence
206 following a well-defined methodology. First, segmentation was performed for every image by calculating

207 a threshold value, which is equal to the minimum digital level in the image plus 15% of the difference
208 between the maximum and the minimum. This percentage was set, based on previous experience, as a
209 compromise to remove light reflected off the liquid spray and the chamber walls without losing much
210 information from the combustion event [29]. After segmentation, the flame area is defined as the
211 summation of the number of pixels which belong to the flame (above the threshold). Thus, the digital
212 levels of all pixels containing the combustion radiation (those above the threshold) are accumulated and
213 averaged over the number of pixels of the flame area obtaining a single mean flame intensity parameter
214 named I_{mean} . Additionally, an apparent combustion velocity (ACV) is calculated as Equation 1 [20], where
215 A is the flame area, L is the perimeter of the flame area and t is the time:

$$216 \quad \text{ACV} = d(A/L)/dt \quad (1)$$

217 **3. BASIS OF GASOLINE PARTIALLY PREMIXED COMPRESSION IGNITION SPARK** 218 **ASSISTED COMBUSTION CONCEPT**

219 As noted above, one of the main drawbacks of the new combustion concepts is to control the
220 combustion phasing as well as cycle-to-cycle variation. The use of gasoline coupled with the spark
221 assistance has been studied in order to minimize the influence of the thermodynamic conditions on the
222 ignition process for CI engines confirming its suitability to improve the cycle-to-cycle control. Figure 4
223 shows the coefficient of variation of IMEP (COV IMEP) versus IMEP for single and double injection tests
224 using gasoline with spark assistance and a batch of single injection tests using gasoline without spark
225 assistance (PPC).

226 On one hand, comparing the single injection cases with and without the use of the spark (points 3, 4 and
227 5) in figure 4, it is possible to state that in all cases the COV IMEP is reduced using the spark assistance.
228 Focusing on low load (point 3), it is possible to observe how the case without spark assistance has an
229 unacceptable COV IMEP. However, by means of the spark assistance COV IMEP is halved in the same
230 operating condition widening the operating range. Unfortunately, for low-medium loads and

231 considering the same fuel injection quantities for points 3, 4 and 5 in figure 4 the IMEP values are
232 decreased due to the nature of this combustion type (less constant volume-like coupled with a longer
233 combustion duration).

234 On the other hand, comparing only single and double injection tests with spark assistance, it is possible
235 to state that the use of the double injection strategy allows to increase the IMEP values with lower fuel
236 injected mass. This, suggests that the fuel consumption will be diminished. In addition, a reduction at
237 the coefficient of variation is also achieved.

238

239 **3.1 Description of the reference case combustion event**

240 The reference cases for the single and double injection strategies will be used to describe the partially
241 premixed compression ignition with spark assistance combustion process. In both cases, the injection
242 pressure was maintained constant at 900 bar, intake O₂ concentration at 19.6% and injected fuel mass
243 at 21 mg/stk. The temporal evolution of the mass flow rate for both strategies is represented in Figure 5.

244

245 Figure 6a shows the crank angle evolution of different variables. From the top to the bottom, the figure
246 shows the mass flow rate, the mean unburned gas temperature, the in-cylinder pressure and the rate of
247 heat released. In all cases, the spark plug discharge was set at Eol and it determines the SoC. Moreover,
248 to further understand the air/fuel mixing process and the equivalence ratio conditions at SoS and
249 autoignition time, an analysis was carried out using a 1-D jet mixing model. Thus, it is possible to
250 understand how the fuel mass is distributed throughout different equivalence ratios as a function of
251 time. By processing the 1-D model results, a distribution of the fuel mass mixture fraction using bins of
252 0.2 ϕ width at experimental SoC and autoignition is obtained. Figure 6b shows, for the single and double
253 injection strategies, the fuel mass mixture distributions calculated using the 1-D jet mixing model
254 described above. Figure 7 and Figure 9 show the temporal evolution of the natural luminosity (NL) and

255 OH radical for the single and double injection reference combustion cycles represented in Figure 6. Each
256 image corresponds to the crank angle degree showed above them. In addition, the spark plug location
257 (SP) and the swirl motion is depicted in the first image of the sequence. In Figure 8, the temporal
258 evolution of the non-dimensional flame area (the flame area divided by the combustion chamber area),
259 the apparent combustion velocity (ACV) and the mean intensity in the combustion chamber are shown
260 for both injection strategies.

261 A detailed description of the PPC Spark Assisted combustion development under single injection
262 conditions will be explained in order to take it as a reference to compare with the double injection
263 strategy. Considering the red color lines in Figure 6a, once the injection process has finished at -9.8 CAD,
264 the spark plug discharge takes place initiating the combustion process. At this time (-9.8 CAD in Figures 7
265 and 9), it is possible to observe that the first kernel near the spark plug presents intensity values above
266 the minimum threshold of the correlated color scale. Therefore, it is confirmed that the start of
267 combustion is controlled by the spark plug and not by the in-cylinder thermodynamic conditions. The
268 kernel growth generates a partially premixed flame propagation. As Figure 6a shows, an almost linear-
269 sustained heat release from -9.8 CAD to -3.5 CAD is attained. The flame propagation is guided by the
270 swirl motion which can be clearly observed along the whole combustion sequence presented in Figure 7.
271 It should be noticed that without the spark assistance the combustion process is not achieved at all
272 under these operating conditions.

273 The energy released during the flame propagation phase described above causes an increase in the
274 unburned gas pressure and temperature (Figure 6a), leading to a second phase of combustion governed
275 by the autoignition of the rest of the mixture from -3.5 CAD to +2.4 CAD. Aside from the increase in the
276 unburned gas pressure and temperature, it is also possible to appreciate this second stage during the
277 combustion development by observing the RoHR profiles in terms of maximum peak (76 J/CAD for the
278 flame propagation and 175 J/CAD for the autoignition) as well as in the combustion duration (7.8 CAD

279 for the flame propagation vs 4.3 CAD for the autoignition) shown in Figure 6a. This second phase is also
280 noticeable observing the changes in the flame pattern shown in the images of Figure 7 and Figure 9. This
281 change in the flame pattern leads to a higher combustion area and luminosity as it can be appreciated in
282 the mean luminosity profile presented in Figure 8. In this sense, another way to confirm that the
283 autoignition phase is faster than the flame propagation phase is the comparison of the ACV peaks of
284 both phases for the single injection strategy in Figure 8.

285 Regarding double injection strategy, the RoHR profile in Figure 6a shows two combustion stages, as well.
286 However, some differences are found comparing with the single injection case. It is possible to
287 appreciate in both, Figure 7 and 9, how the first kernel near the spark plug (-2.3 CAD) is fainter than the
288 one acquired in the single injection case (-9.8 CAD). The luminosity is related with the mixture
289 distribution at SoC shown in Figure 6b. The comparison of the mixture distributions for both strategies
290 reveals clear differences in the distribution of the fuel mass at SoC. Two zones are observed in the
291 double injection strategy. The first zone ($0.2 < \phi < 0.8$) is attributed to the fuel injected during the pilot
292 injection. In this zone, the fuel mass is distributed under low equivalences ratios because of the longer
293 mixing time provided by the dwell between the injections. In the second zone ($\phi > 0.8$), attributed to the
294 main injection, the fuel mass is distributed under more reactive equivalences ratios providing the local
295 conditions needed to ignite the mixture with the spark plug assistance. Comparing the mixture
296 distributions for both strategies at SoC, it can be appreciated how the single injection strategy leads a
297 considerably higher amount of fuel mass mixed up to rich equivalence ratios in comparison with the
298 double injection strategy. Particularly, the more fuel mixed in this range of equivalence ratios (from
299 $\phi = 0.5$ to $\phi = 3.5$) ensures that some part of the mixture distribution is inside the range of flammability
300 limits. Therefore, the spark is capable of promoting the start of combustion and the progression of the
301 premixed flame. This higher quantity of fuel mass under stoichiometric and rich equivalences ratios in
302 the case of the single injection strategy becomes in a first kernel with high temperature once the spark

303 plug has discharged the energy. It is possible to confirm the higher temperature in the case of the single
304 injection by comparing the OH radical luminosity in single injection strategy (-9.8 CAD) and double
305 injection strategy (-2.3 CAD) in Figure 9. Thus, comparing the mean intensity profiles shown in Figure 8,
306 it can be noticed that the flame intensity in the kernel (just after the peak observed during the spark
307 discharge) in the double injection strategy is lower than in a single injection strategy (220 a.u. vs 128
308 a.u.).

309 Considering the comparison between flame propagation phases for single and double injection
310 strategies, it can be stated that the flame propagation phase in the double injection strategy from -2.3
311 CAD to +7.6 CAD in Figures 7 and 9 is slower and less intense than in the single injection case. It can be
312 confirmed taking into account the lower ACV peak in the double injection (at +2.2 CAD) compared with
313 the single injection case (at -6.8 CAD) in Figure 8, as well as the maximum RoHR values obtained during
314 this phase (double injection: 60 J/CAD versus single injection: 77 J/CAD) in Figure 6a. Both parameters,
315 apparent combustion velocity and heat release, are highly related with the in-cylinder local equivalence
316 ratio distribution. Figure 6b shows a lower amount of fuel mass within the range of reactive conditions
317 in the double injection case, slowing down the flame propagation. This slowing down can be observed
318 comparing the RoHR duration in both injection strategies attributed to the flame propagation phase in
319 Figure 6a (9 CAD for the double injection vs 7 CAD for the single injection). These differences in the
320 equivalence ratio distribution can be also noticed in Figure 7 by means of the luminosity acquired in the
321 first instants of the flame propagation phase. Taking into account the color scale in Figure 7, the
322 luminosity obtained in the single injection (from -6.4 CAD to -3.5 CAD) is more intense than in the
323 double injection case (from +2.2 CAD to +5.1 CAD). This fact is ratified comparing both mean intensity
324 profiles in Figure 8. By contrast, due to the more homogeneous fuel-air distribution attained with the
325 pilot injection, a larger area is covered in the case of the double injection during this period as Figure 8
326 shows.

327 Once the flame propagation phase has been compared between both injection strategies, the
328 differences found during the autoignition time are explained. At the autoignition time, the fuel mass
329 distributions presented in Figure 6b are quite similar in both injection strategies. The extra mixing time
330 (around 8 CAD in both cases) achieved from the Eol up to the autoignition time provides a leaner and
331 more homogeneous in-cylinder mixture distribution. This homogeneity in the mixture, together with the
332 increase in the in-cylinder pressure and temperature due to the first combustion phase, promotes a
333 faster combustion development during this autoignition phase compared with the flame propagation
334 phase. Comparing the mixture distributions in both injection strategies, it is possible to appreciate that
335 in both cases all the mixture is distributed below the stoichiometric equivalence ratio being the more
336 remarkable difference the higher fuel mass amount available in the double injection strategy. It
337 promotes a more powerful and faster autoignition compared with the single injection strategy. In the
338 same way, it is possible to confirm this behavior making a comparison between the maximum RoHR
339 peaks in Figure 6a (268 J/CAD versus 176 J/CAD in the single injection case) as well as comparing the
340 autoignition phase ACV peaks in both injection strategies (at -5 CAD in single injection and +4.8 CAD in
341 double injection) in Figure 8. It is interesting to note that the double injection strategy improves the
342 region where the combustion takes place, covering the whole combustion chamber. This can be clearly
343 confirmed by looking the non-dimensional flame area profile depicted in Figure 8, as well as comparing
344 the images of Figure 7 (single injection: +2.4 CAD vs double injection: +9.1 CAD or single injection: +5.6
345 CAD vs double injection: +10.1 CAD).

346 **4. CONCLUSIONS**

347 The influence of the double injection strategy on the Spark Assisted Partially Premixed Compression
348 Ignition combustion concept fuelled with high ON gasoline at low load operating conditions has been
349 studied combining theoretical and practical tools. An analysis of the parameters derived from in-cylinder
350 pressure measurement has been combined with the 1-D jet model calculations. In order to complement

351 the research, images of the natural luminosity and OH radical as well as different parameters derived
352 from these images have been also analysed.

353 The spark assistance with double injection strategy has been found to be capable of extending the limits
354 of the gasoline CI combustion mode at low-medium load conditions to lower fuelling levels than was
355 possible with single injection strategy. Another important finding obtained by means of the in-cylinder
356 images acquired with the high speed cameras is that the spark assistance is capable to provide spatial
357 and temporal control over the combustion process in the double injection strategy conditions tested.
358 Regarding the general development of the combustion process, the combustion phenomenology
359 described here is consistent with previous Spark Assisted PPC work using a single injection strategy. The
360 spark plug discharge takes place initiating the combustion process by means of a first kernel. The kernel
361 growth generates a partially premixed flame propagation that rises the unburned gas pressure and
362 temperature leading to a second phase of combustion governed by the autoignition of the rest of the
363 mixture. Important differences on the different combustion phases have been found in the double
364 injection operating conditions tested:

- 365 - A fainter *kernel* is produced due to the leaner equivalence ratios at SoC. This leaner
366 equivalence ratio distribution, presented by the 1-D jet model calculations, results in a lower in-
367 chamber luminosity (mean natural luminosity) and temperature (OH radical).
- 368 - The leaner mixture conditions during the first instants of the combustion development makes
369 the *flame propagation phase* of the double injection strategy slower compared with the single
370 injection strategy, as the apparent combustion velocity values shows. That is also possible to
371 appreciate by comparing the RoHR durations. This leaner equivalence ratio distribution results
372 in a lower in-chamber luminosity (mean natural luminosity) and temperature (OH radical). In

373 addition, the double injection strategy is less energetic than the single injection case as the
374 comparison of the maximum peaks of the RoHR denotes.

375 - With reference to the *autoignition* phase, the improvement in the spatial mixture distribution
376 associated to the pilot injection improves the region in which the combustion takes place,
377 covering the whole combustion chamber. It has been demonstrated with the images acquired as
378 well as with the non-dimensional area calculation. Due to the higher mixture amount available
379 to be burned at this time, a more intense autoignition is attained (higher maximum RoHR peak).
380 In addition, it is possible to appreciate higher maximum peaks in the apparent combustion
381 velocity besides a lower RoHR duration.

382 It is interesting to remark that the use of the double injection strategy allows an increase in the IMEP
383 values with lower fuel injected mass. In addition, a reduction of the coefficient of variation is obtained.
384 Thus, a reduction in the fuel consumption is expected.

385 **ACKNOWLEDGMENTS**

386 The authors would like to thank General Motors for supporting this research.

387 **REFERENCES**

- 388 [1] Yanagihara H, Sato Y, Minuta J. A simultaneous reduction in NO_x and soot in diesel engines under a
389 new combustion system (Uniform Bulky Combustion System e UNIBUS), in: 17th International
390 Vienna Motor Symposium, pp. 303-314, 1996.
- 391 [2] Wu H-W, Wang R-H, Ou D-J, Chen Y-C, Chen T-Y. Reduction of smoke and nitrogen oxides of a partial
392 HCCI engine using premixed gasoline and ethanol with air. Applied Energy, Vol. 88, pp 3882-3890,
393 2011.
- 394 [3] Akagawa H, Miyamoto T, Harada A , Sasaki S, et al. Approaches to Solve Problems of the Premixed
395 Lean Diesel Combustion. SAE Technical Paper 1999- 01-0183, 1999.

- 396 [4] Kimura S, Aoki S, Kitahara Y, Aiyoshizawa E. Ultra-clean Combustion Technology Combining a Low-
397 temperature and Premixed Combustion Concept for Meeting Future Emission Standards, SAE
398 International, SAE 2001-01-0200, 2001.
- 399 [5] Maurya R K, Agarwal A K. Experimental study of combustion and emission characteristics of ethanol
400 fuelled port injected homogeneous charge compression ignition (HCCI) combustion engine. Applied
401 Energy, Vol. 88, pp 1169-1180, 2011.
- 402 [6] Lu X, Han D, Huang Z. Fuel design and management for the control of advanced compression-
403 ignition combustion modes. Progress in Energy and Combustion Science, 37, 2011:741-783.
- 404 [7] Mingfa Y, Zhaolei Z, Haifeng L. Progress and recent trends in homogeneous charge compression
405 ignition (HCCI) engines. Progress in Energy and Combustion Science 35 (5) (October 2009) 398-437.
- 406 [8] Cerit M, Soyhan HS. Thermal analysis of a combustion chamber surrounded by deposits in an HCCI
407 engine. Applied Thermal Engineering 50 (1) (2013) 81-88.
- 408 [9] Kiplimo R, Tomita E, Kawahara N, Yokobe S. Effects of spray impingement, injection parameters, and
409 EGR on the combustion and emission characteristics of a PCCI diesel engine, Applied Thermal
410 Engineering 37 (May 2012) 165-175.
- 411 [10] Singh AP, Agarwal AK. Combustion characteristics of diesel HCCI engine: an experimental
412 investigation using external mixture formation technique. Appl Energy 2012.
- 413 [11] Law D, Kemp D, Allen J, Kirkpatrick G, Copland T. Controlled combustion in an IC-engine with a fully
414 variable valve train. SAE paper 2001-01-0251; 2001.
- 415 [12] Agrell F, Ångström H-E, Eriksson B, Wikander J, Linderyd J. Integrated simulation and engine test of
416 closed loop HCCI control by aid of variable valve timings. SAE paper 2003-01-0748; 2003.
- 417 [13] Haraldsson G, Tunestål P, Johansson B, Hyvönen J. HCCI combustion phasing in a multi cylinder
418 engine using variable compression ratio. SAE paper 2002-01-2858; 2002.

- 419 [14]Maurya R K, Agarwal A K. Experimental investigation on the effect of intake air temperature and air–
420 fuel ratio on cycle-to-cycle variations of HCCI combustion and performance parameters. Applied
421 Energy, Vol. 88, pp 1153-1163, 2011.
- 422 [15]Yang J, Culp T, Kenney T. Development of a Gasoline Engine System Using HCCI Technology e the
423 Concept and the Test Results, SAE paper 2002-1-2832.
- 424 [16]Kalghatgi GT, Kumara Gurubaran R, Davenport A, Harrison AJ, Hardalupas Y, Taylor AMKP. Some
425 advantages and challenges of running a Euro IV, V6 diesel engine on a gasoline fuel. Fuel, Vol. 108,
426 pp 197-207, 2013.
- 427 [17]Yu C, Wang J, Wang Z, Shuai S. Comparative study on Gasoline Homogeneous Charge Induced
428 Ignition (HCII) by diesel and Gasoline/Diesel Blend Fuels (GDBF) combustion. Fuel, Vol. 106, pp 470-
429 447, 2013.
- 430 [18]Lewander CM, Johansson B, Tunestal P. Extending the Operating Region of Multi-Cylinder Partially
431 Premixed Combustion using High Octane Number Fuel. SAE Paper 2011-01-1394; 2011.
- 432 [19]Persson H, Rémon A, Hultqvist A, Johansson B. Investigation of the Early Flame Development in
433 Spark Assisted HCCI Combustion Using High Speed Chemiluminescence Imaging, SAE 2007-01-0212.
- 434 [20]Persson H, Rémon A, Johansson B. The Effect of Swirl on Spark Assisted Compression Ignition (SACI).
435 JSAE 20077167, SAE 2007-01-1856; 2007.
- 436 [21]Wang Z, Shuai SJ, Wang JX, Tian G-H, Ma Xinliang QJ. Study of the effect of spark ignition on gasoline
437 HCCI combustion. Proceedings of the Institution of Mechanical Engineers, Part D: Journal of
438 Automobile Engineering. <http://dx.doi.org/10.1243/09544070JAUTO151>.
- 439 [22]Natajara VK, Volker S, Reuus DL, Silvas G. Effect of sparkignition on combustion periods during
440 spark assisted compression ignition. Combust Sci Technol 2009;181:1187–206.

- 441 [23]Desantes JM, Payri R, García A, Monsalve-Serrano J. Evaluation of Emissions and Performances from
442 Partially Premixed Compression Ignition Combustion using Gasoline and Spark Assistance. SAE paper
443 2013-01-1664; 2013.
- 444 [24]Benajes J, García A, Domenech V, Durrett R. An investigation of partially premixed compression
445 ignition combustion using gasoline and spark assistance. Applied Thermal Engineering Vol 52 p. 468–
446 477; 2013.
- 447 [25]Lapuerta M, Armas O, Hernández JJ. Diagnostic of D.I. Diesel Combustion from In-Cylinder Pressure
448 Signal by Estimation of Mean Thermodynamic Properties of the Gas. Applied Thermal Engineering.
449 Vol 19 N° 5 p. 513–529; 1999.
- 450 [26]Payri F, Molina S, Martín J, Armas O. Influence of measurement errors and estimated parameters on
451 combustion diagnosis. Applied Thermal Engineering Vol 26 N° 2-3 p. 226–236; 2006.
- 452 [27]Pastor JV, López JJ, García JM, Pastor JM. A 1D model for the description of mixing-controlled inert
453 diesel sprays. SAE paper 2005-01-1126; 2005.
- 454 [28]Desantes JM, Pastor JV, García-Oliver JM, Pastor JM. A 1D model for the description of mixing-
455 controlled reacting diesel sprays. Combustion and Flame 2009; 156:234–49.
- 456 [29]Pastor JV, Bermúdez V, García-Oliver JM, Ramírez-Hernández JG. Influence of spray-glow plug
457 configuration on cold start combustion for high-speed direct injection diesel engines. Energy 36
458 (2011) 5486-5496.

459

460 **ABBREVIATIONS**

461 ASTM: American Society of Testing Materials

462 bTDC: before Top Dead Center

463 BDC: Bottom Dead Center

464 CAD: Crank Angle Degree

465 CI: Compression Ignition

466 CMOS: Complementary Metal Oxide Semiconductor
467 COV: Coefficient Of Variation
468 DI: Direct Injection
469 EOI_{main} : End of main injection
470 EOI_{pilot} : End of pilot injection
471 EVO: Exhaust Valve Opening
472 FeCE: Fuel energy Conversion Efficiency
473 HCCI: Homogeneous Charge Compression Ignition
474 IVC: Intake Valve Closing
475 IMEP: Indicated Mean Effective Pressure
476 LTC: Low Temperature Combustion
477 ON: Octane Number
478 PCCI: Premixed Charge Compression Ignition
479 PID controller: Proportional-Integral-Derivative controller
480 PPC: Partially Premixed Charge
481 SOI_{main} : Start of main injection
482 SOI_{pilot} : Start of pilot injection
483 SoC: Start of Combustion
484 SoS: Start of Spark
485 TDC: Top Dead Center

486

487 **HIGHLIGHTS**

- 488 - Double injection improves the combustion control in low load.
- 489 - Double injection enhances both phases of the combustion mode.

- 490 - Double injection increases the combustion area in the chamber.
- 491 - Combustion process described by mixing process, OH* and natural luminosity images.

492

493

494

495

496 **Tables**

497

Type	CI, 4stroke, DI
Max. engine speed [rpm]	4500
Cylinder number	1
Displacement [cm³]	544.75
Bore [mm]	85
Stroke [mm]	96
Compression ratio [-]	14.7:1
Bowl diameter [mm]	45
Bowl depth [mm]	18
Bowl volume [cm³]	25

498

499 Table 1. Main single cylinder engine characteristics

500

	Gasoline
Density (T=15°C) [kg/m³]	722
Viscosity (T=40°C) [mm²/s]	0.37
RON [-]	98
Lower heating value [kJ/kg]	44542

501

502 Table 2. Characteristics of the gasoline used in the study

503

Type	Common-Rail
Injector	Bosch CRIP 3.3
Hole number	7
Included angle [deg]	154°
Hole diameter [um]	97 um

Flow capacity [cm ³ /30s]	210
--------------------------------------	-----

504
505
506
507
508
509
510
511
512
513
514
515
516
517
518
519
520
521
522
523
524
525
526
527
528
529
530
531
532

Table 3. Injection system characteristics used in the study

Figure captions

- Figure 1. Complete test cell setup
- Figure 2. Image of the modified cylinder head with spark plug and injector hole (left). Diagram of the relative position between the injector and spark plug (right)
- Figure 3. Optical configuration for the image acquisition
- Figure 4. IMEP vs. COV IMEP for single and double injection strategy and cases with and without spark assistance
- Figure 5. Single and double injection strategy mass flow rate for the reference cases
- Figure 6. Crank angle evolution of the mass flow rate, unburned gas temperature, in-cylinder pressure, and rate of heat released for the single injection strategy and double injection strategy (6a). Distribution of fuel mass vs. φ in experimental SoS and autoignition time for the single and double injection strategies (6b).
- Figure 7. Temporal evolution of the natural luminosity (NL) for the reference combustion cycle for the single injection (upper) and double injection (lower). Each image corresponds to the crank angle degree showed above them
- Figure 8. Temporal evolution of the non-dimensional flame area, apparent flame velocity and mean flame intensity for the single (red lines) and double (blue lines) injection cases presented above
- Figure 9. Temporal evolution of the OH radical luminosity for the reference combustion cycle for the single injection (upper) and double injection (lower) cases. Each image corresponds to the crank angle degree shown above them

533

534

535

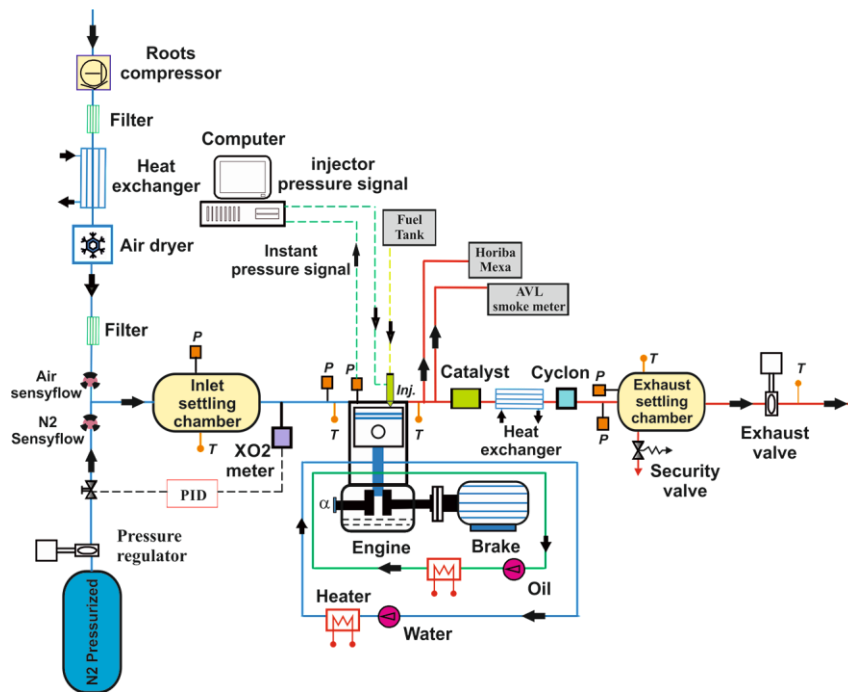
536

537

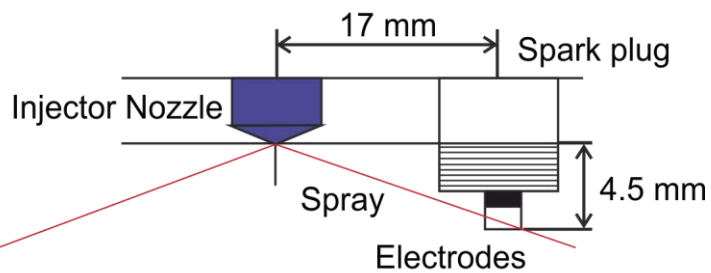
538

539

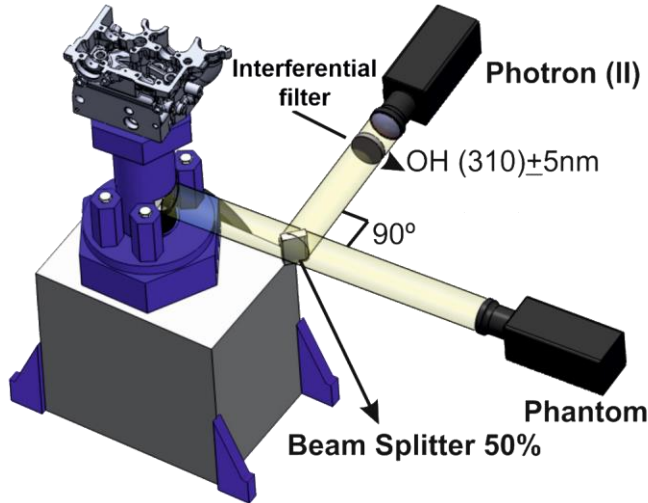
540 **Figures**



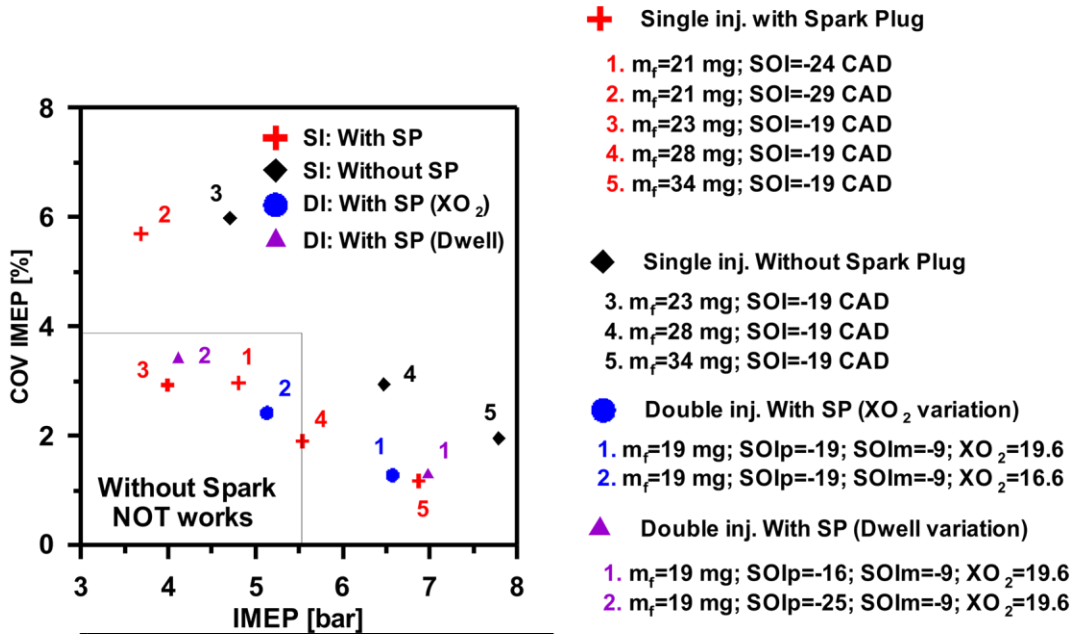
541



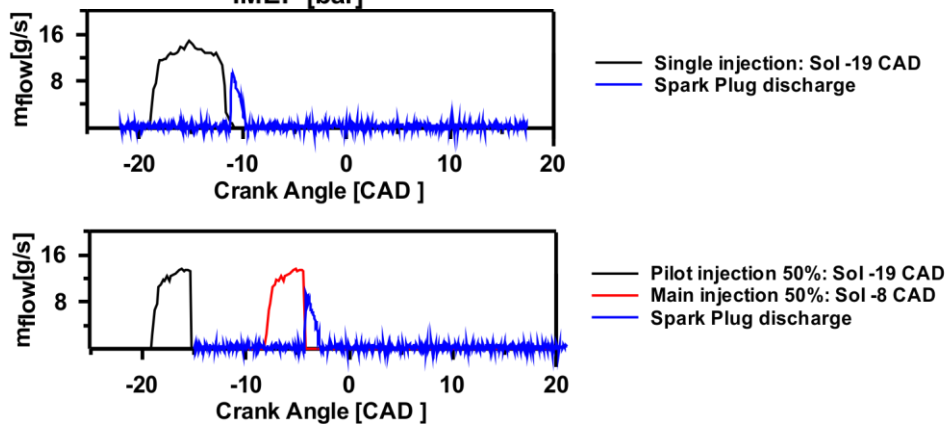
542



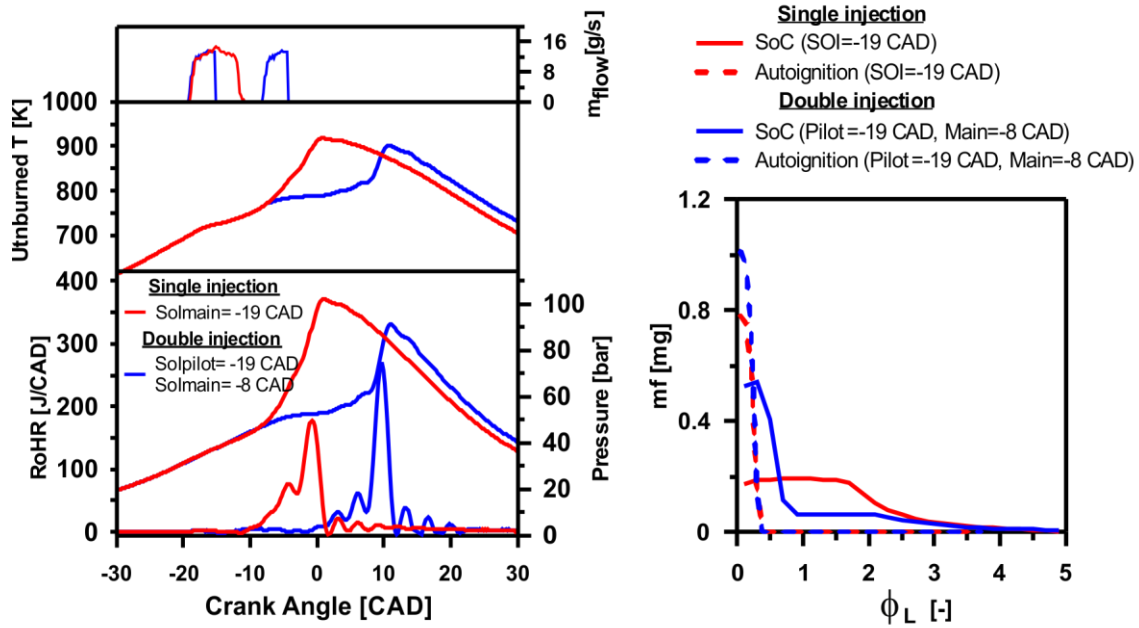
543



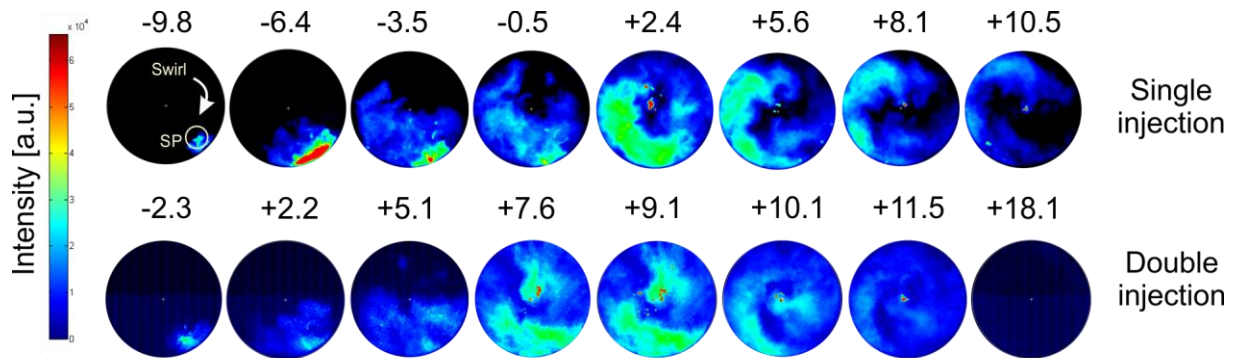
544



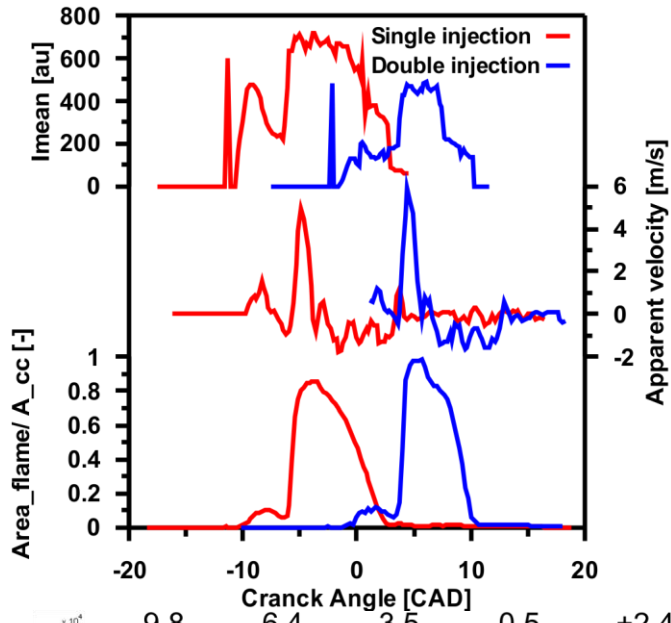
545



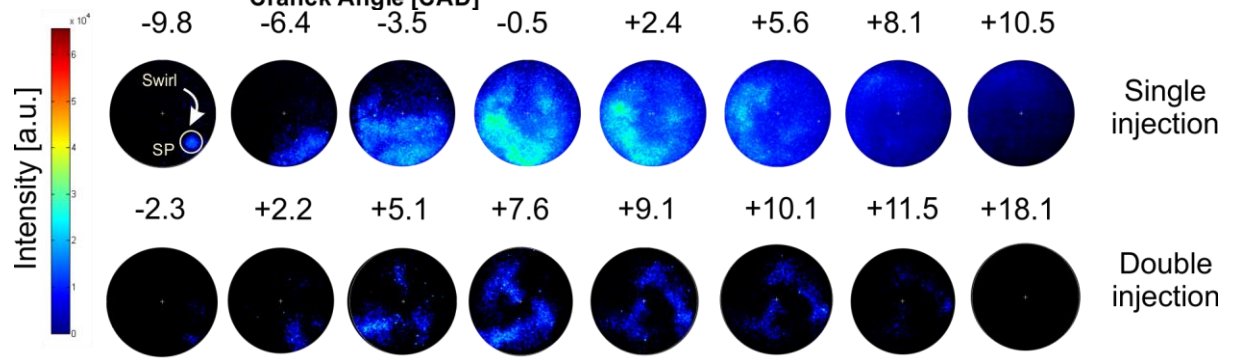
546



547



548



549